A Model of Spatial Epidemic Spread When Individuals Move within Overlapping Home Ranges

Timothy C. Reluga*, Jan Medlock, Alison P. Galvani

Department of Epidemiology and Public Health, Yale University School of Medicine, New Haven, CT 06520

Abstract One of the central goals of mathematical epidemiology is to predict disease transmission patterns in populations. Two models are commonly used to predict spatial spread of a disease. The first is the distributed-contacts model, often described by a contact distribution among stationary individuals. The second is the distributed-infectives model, often described by the diffusion of infected individuals. However, neither approach is ideal when individuals move within home ranges. This paper presents a unified modeling hypothesis, called the restricted-movement model. We use this model to predict spatial spread in settings where infected individuals move within overlapping home ranges. Using mathematical and computational approaches, we show that our restricted-movement model has three limits: the distributed-contacts model, the distributed-infectives model, and a third, less studied advective distributed-infectives limit. We also calculate approximate upper bounds for the rates of an epidemic's spatial spread. Guidelines are suggested for determining which limit is most appropriate for a specific disease.

Keywords Epidemics · Invasions · Distributed-contacts · Distributed-infectives

1. Introduction

A fundamental challenge in mathematical epidemiology is determining how the structure of a population influences disease transmission. One important aspect is the spatial structure. For instance, the SARS epidemic spread through 12 countries within a few weeks. Projections of the spatial spread of an epidemic and the interactions of human movement at multiple levels with a response protocol will facilitate the assessment of policy alternatives. Spatially-explicit models are necessary to evaluate the efficacy of movement controls (Riley et al., 2003; Eubank et al.,

---

*Corresponding author.
E-mail address: timothy.reluga@yale.edu (Timothy C. Reluga).

2004). Models that ignore spatial structure can lead to inaccuracy in the prediction of population dynamics (Durrett and Levin, 1994).

A wide variety of methods have been used for the study of spatially structured epidemics. Some examples include cellular automata (Doran and Laffan, 2005; Fuks and Lawniczak, 2001), networks (Bauch and Galvani, 2003; Newman, 2002), metapopulations (Lloyd and Jansen, 2004; Arino and van den Driessche, 2003; Keeling and Gilligan, 2000), individual-based models (Bian, 2004), moment-closure approximations (Thomson and Ellner, 2003; Filipe and Maule, 2003), interacting particle systems (Durrett, 1999; Schinazi, 1996), diffusion equations (Caraco et al., 2002; Méndez, 1998), integro-differential equations (Medlock and Kot, 2003), and integrodifference equations (Allen and Ernest, 2002). Two particularly useful approaches for describing a disease's rate of spatial spread are the distributed-contacts and distributed-infectives models.

Kendall (1965) and Mollison (1972) developed the theory of asymptotic spread rates in distributed-contacts models. Their family of integral-equation models assumed that each individual is stationary and has a distribution of contacts over space (Mollison, 1972). Distributed-contacts models are particularly appropriate for the study of plant diseases (van den Bosch et al., 1988; Metz and van den Bosch, 1995; van den Bosch et al., 1999), but researchers are also using the closely related framework of contact networks to study disease transmission in human populations (Newman, 2002; Meyers et al., 2005; Read and Keeling, 2003).

Shortly after Mollison's first work, Noble (1974) formulated the closely related theory of asymptotic spread rates under the distributed-infectives model. Building on earlier work tracing back to Fisher and Kolmogorov, Noble applied diffusion theory to the spread of bubonic plague in Europe (Noble, 1974). Noble's model relies on the assumptions that disease is transmitted through interactions between dispersing individuals, and that infected individuals move in uncorrelated random walks. Medlock and Kot (2003) recently developed a distributed-infectives framework that uses a flexible kernel-based approach similar to that employed in earlier distributed-contact models. They found that inappropriate application of either the distributed-contact or distributed-infectives approaches can generate inaccurate projections of epidemic spread.

In many epidemiological contexts, the transmission process involves components of both distributed contacts and distributed infectives. Hybrid models have been proposed for this situation. For instance, the equation of Bailey (1975),

$$\frac{\partial n}{\partial t} = r\left(n + D_{DC}\nabla^2 n\right) + D_{DI}\nabla^2 n - \mu n, \tag{1}$$

allows for both diffusive contacts and diffusive movement. An analogous spatially non-local model,

$$\frac{\partial n}{\partial t} = r\left(\int_\Omega k_{DC}(x, y)n(y, t)\mathrm{d}y\right) + \int_\Omega k_{DI}(x, y)\left[n(y, t) - n(x, t)\right]\mathrm{d}y - \mu n, \tag{2}$$

incorporates both a movement kernel k_{DI} and a contact kernel k_{DC}. Busenberg and Travis (1983) study a related model with diffusive movement of individuals and

distributed contacts. Recent study of a model where individuals transition between stationary and motile states (Hadeler, 2003) demonstrates that both distributed-infectives and distributed-contacts models can appear as limiting cases of a single model.

Spatially structured epidemic models are useful tools in the study of geographic epidemic spread. In particular, spatial models can be used to estimate the speed of geographic spread. Estimates of rapidity of disease dissemination can, in turn, be used to guide policy decisions. For many linear models, such as the one discussed in this paper, researchers have shown that there is a minimum speed c^* for traveling wave solutions and that in many biologically realistic settings, solutions tend to approach advancing fronts that travel no faster than c^*. The speed of advancing fronts in non-linear deterministic and linear stochastic models has been shown in a number of instances to be given by the minimum speed c^* from a corresponding linear model (Mollison, 1991; Kot et al., 2004). The connection between speeds of non-linear models with their corresponding linear models holding more generally is the subject of the "linear conjecture" (van den Bosch et al., 1990; Mollison, 1991). Moreover, the minimum speed from a linear model often provides a good upper bound for the speeds observed in non-linear stochastic models (Mollison, 1972; McKean, 1975; Mollison, 1977; Lewis, 2000; Lewis and Pacala, 2000; Clark et al., 2001; Snyder, 2003).

Here we consider a scenario that does not neatly conform to the assumptions of either the distributed-contacts or distributed-infectives hypotheses: the case of individuals moving within overlapping home ranges. Many animal species live within a "home range" and periodically return to their "home." We develop a restricted-movement model that describes movement relative to a "home" location, and study the rate of spatial spread of disease using mathematical analysis and stochastic simulations. We show that the restricted-movement model possesses limits corresponding to the distributed-contact and distributed-infective models, but also possesses a third limit, which we call the advective distributed-infectives model. Approximations to the rate of spread are provided in all three limits. These approximations agree with the speeds observed in individual-based Monte Carlo simulations in all but the advective distributed-infectives limit.

2. Restricted-movement model

Consider a large population distributed uniformly over a one-dimensional world. Every individual has a spatial position, denoted by x, and a "home" location, denoted by x_h. An individual's home remains constant, but the individual's position changes according to a biased random walk over time. Specifically, we assume that an individual is attracted to its home with a force proportional to its current displacement from that home, $x - x_h$. Given an initial position y, the probability density $p(x|y, x_h, t)$ for the individual's position at time t satisfies the partial differential equation

$$\frac{\partial p}{\partial t} = D \frac{\partial^2 p}{\partial x^2} + \alpha \frac{\partial}{\partial x} \left[(x - x_h) p \right], \tag{3}$$

with delta-function initial condition

$$p(x|y, x_h, 0) = \delta(x - y), \tag{4}$$

where D is the rate of diffusion, and α is the strength of attraction of the individuals towards their homes. Eqs. (3) and (4) have solution

$$p(x|y, x_h, t) = \frac{1}{\sqrt{2\pi(1 - e^{-2\alpha t})D/\alpha}} \exp\left\{\frac{-\alpha\left[(x - x_h) - (y - x_h)e^{-\alpha t}\right]^2}{2D(1 - e^{-2\alpha t})}\right\}. \tag{5}$$

As time passes, the probability distribution of the individual's position approaches the stationary Gauss distribution

$$p(x|y, x_h, t = \infty) = \frac{1}{\sqrt{2\pi D/\alpha}} \exp\left[\frac{-\alpha(x - x_h)^2}{2D}\right]. \tag{6}$$

Every individual is restricted to a neighborhood with variance D/α. This general description of the random motion of an elastically confined particle is given by an Ornstein–Uhlenbeck process (Uhlenbeck and Ornstein, 1930; Goel and Richter-Dyn, 1974).

Now consider the introduction and transmission of an infectious disease. Let $n(x, x_h, t)$ be the density of infected individuals at position x with home x_h at time t. Individuals may behave differently depending on whether they are infected or susceptible. Therefore, let D_i and α_i describe the diffusion and attraction of infected individuals, and let D_s and α_s describe the diffusion and attraction of susceptible individuals. Let transmission of infection occur only among individuals occupying the same position x. If susceptible individuals have been dispersing for a long time ($\gg 1/\alpha_s$) prior to the introduction of infection, the density of susceptible individuals with homes x_h, as given by Eq. (6), is

$$\frac{e^{-\alpha_s(x - x_h)^2/2D_s}}{\sqrt{2\pi D_s/\alpha_s}}. \tag{7}$$

It follows that the rate at which newly infected individuals with home x_h appear at position x at time t is

$$r\frac{e^{-\alpha_s(x - x_h)^2/2D_s}}{\sqrt{2\pi D_s/\alpha_s}}\int_{-\infty}^{\infty} n(x, x_h, t)\,dx_h, \tag{8}$$

where r is the rate of transmission per infection. This is an approximation valid for the earliest phase of an epidemic when the number of susceptibles is not significantly reduced by infection. Infected individuals are removed from the disease dynamics by death, recovery, vaccination or quarantine at a rate μn.

The rate of change in the density $n(x, x_\mathrm{h}, t)$ is the sum of movement under the Ornstein–Uhlenbeck process and new transmissions minus removal,

$$\frac{\partial n}{\partial t} = D_i \frac{\partial^2 n}{\partial x^2} + \alpha_i \frac{\partial}{\partial x}[(x - x_\mathrm{h})n] + r \frac{\mathrm{e}^{-\alpha_\mathrm{s}(x-x_\mathrm{h})^2/2D_\mathrm{s}}}{\sqrt{2\pi D_\mathrm{s}/\alpha_\mathrm{s}}} \int_{-\infty}^{\infty} n \, \mathrm{d}x_\mathrm{h} - \mu n. \tag{9}$$

The restricted-movement model for epidemic spread is posed explicitly by Eq. (9).

Alternatively, the transmission pattern of the restricted-movement model can be posed as a convolution over the density of newly infected individuals $b(y, t)$. Equation (5) provides the probability that an infected individual will be located at position x, conditioned on the location at the time of infection, home location, and time. The conditional dependence on home location can be removed using the definition of conditional probability,

$$p(x|y, t) = \int_{-\infty}^{\infty} p(x|y, x_\mathrm{h}, t)p(x_\mathrm{h}|y) \, \mathrm{d}x_\mathrm{h}. \tag{10}$$

From Eq.(7), we obtain the conditioned distribution of home locations

$$p(x_\mathrm{h}|y) = \frac{\mathrm{e}^{-\alpha_\mathrm{s}(y-x_\mathrm{h})^2/2D_\mathrm{s}}}{\sqrt{2\pi D_\mathrm{s}/\alpha_\mathrm{s}}}. \tag{11}$$

Thus, Eq. (10) is a convolution of Gauss distributions. After integration, we find $p(x|y, t) = A(x - y, t)$, where $A(x, t)$ is also a Gauss distribution in x with mean 0 and time-dependent variance given by

$$(1 - \mathrm{e}^{-2\alpha_i t})\frac{D_i}{\alpha_i} + (1 - \mathrm{e}^{-\alpha_i t})^2 \frac{D_\mathrm{s}}{\alpha_\mathrm{s}}. \tag{12}$$

The density of newly infected individuals can now be constructed by generalizing the Lotka integral equation (Kot, 2001) to include space. The rate at which all individuals infected at location y' at time $t - \tau$ produce new infections at location y at time t is proportional to the fraction of individuals occupying location y and remaining infected at time t. Integrating over all locations of infection and past times, the density of individuals $b(y, t)$ newly infected at location y at time t will be

$$b(y, t) = r \int_0^t \int_{-\infty}^{\infty} A(y - y', \tau)b(y', t - \tau) \mathrm{e}^{-\mu\tau} \, \mathrm{d}y' \, \mathrm{d}\tau + G(y, t), \tag{13}$$

where $G(y, t)$ is an inhomogeneity corresponding to initial conditions.

3. Analysis

Although the restricted-movement model is linear, spatially-dependent coefficients and non-local terms make Eq. (9) difficult to analyze. Fortunately, the convolution form of Eq. (13) is amenable to analysis using standard transform

methods (Metz et al., 1999). The minimum speed c^* of solutions to the restricted-movement model must satisfy the system

$$\hat{b}(c^*, \omega^*) = 1, \tag{14}$$

$$\frac{\partial \hat{b}}{\partial \omega}(c^*, \omega^*) = 0, \tag{15}$$

where

$$\begin{aligned}
\hat{b}(c, \omega) &= \int_0^\infty \int_{-\infty}^\infty \mathrm{e}^{-\omega(y+ct)} b(y, t)\, \mathrm{d}y\, \mathrm{d}t \\
&= \frac{r}{\alpha_i} \int_0^1 u^{\frac{c\omega+\mu}{\alpha_i}-1} \mathrm{e}^{\frac{1}{2}\omega^2 \left[\frac{D_s}{\alpha_s}(1-u)^2 + \frac{D_i}{\alpha_i}(1-u^2) \right]}\, \mathrm{d}u
\end{aligned} \tag{16}$$

after converting the infinite-domain integral into a finite-domain integral for numerical computation. Heuristically, this approach is equivalent to assuming travelling wave solutions of the form $b(y, t) = \exp[-\omega(y + ct)]$, deriving a dispersion relation $c(\omega)$, and then using comparison theory (Fife, 1979) to argue that solutions originating from compact initial conditions will travel with asymptotic speed $c^* = \min_\omega c(\omega)$.

Numerical solutions of Eqs. (14) and (15) can describe the rate of spread under different parameter regimes. For instance, Fig. 1 shows that the qualitative effect of removal on the speed of epidemic spread is independent of α. When $\mu \ll r$, the decrease in the asymptotic speed of spread is proportional to μ, and as removal rate μ approaches the transmission rate r, the speed vanishes with $c^* \propto \sqrt{1 - \mu/r}$. This relation can be derived analytically by using a two-term Taylor approximation for the exponential in the integrand of Eq. (16) when ω is small. This yields

$$c^*_{\mathrm{EX}} \approx 2r \sqrt{\frac{\left(1 - \frac{\mu}{r}\right)\left(\frac{D_s}{\alpha_s} + \frac{D_i}{\alpha_i} + \frac{rD_i}{\alpha_i^2}\right)}{\left(1 + \frac{r}{\alpha_i}\right)\left(2 + \frac{r}{\alpha_i}\right)}}. \tag{17}$$

To better understand the mechanisms involved, we will study the rate of spread in the remaining three limiting cases depicted in Fig. 2. The heuristic arguments we provide can also be made in a more formal manner by the careful study of Eq. (13).

3.1. Distributed-contacts limit

When the homeward attraction is much larger than the transmission rate ($r \ll \alpha_i$), the position of each infected individual is reasonably approximated by the time-independent solution of the Ornstein–Uhlenbeck equation. Using a separation-of-variables ansatz, we let

$$n(x, x_{\mathrm{h}}, t) = \frac{\mathrm{e}^{-\alpha_i(x-x_{\mathrm{h}})^2/2D_i}}{\sqrt{2\pi D_i/\alpha_i}} \tilde{n}(x_{\mathrm{h}}, t). \tag{18}$$
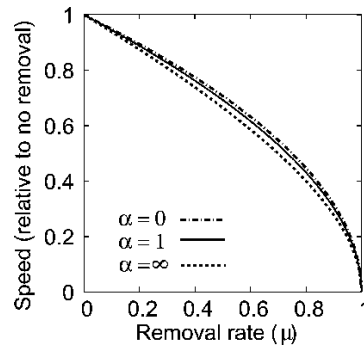
Fig. 1 Proportional decreases in the spread rate c^* depending on the removal rate μ compared to cases of no removal ($\mu = 0$), as calculated from Eqs. (14) and (15). Faster removal rates μ of infected individuals slow the spread of infection in a similar fashion for different values of α. Parameters: $r = 1$, $D_s/\alpha_s = D_i/\alpha_i = 1$, $\alpha_i = \alpha_s = \alpha$.

Substituting Eq. (18) into Eq. (9) and integrating over all space x, we find $\tilde{n}$ is governed by the integro-differential equation

$$\frac{\partial \tilde{n}(x_h, t)}{\partial t} = r \left[2\pi \left(\frac{D_i}{\alpha_i} + \frac{D_s}{\alpha_s} \right) \right]^{-1/2} \int_{-\infty}^{\infty} e^{-(x_h - u)^2 \left(\frac{2D_i}{\alpha_i} + \frac{2D_s}{\alpha_s} \right)^{-1}} \tilde{n}(u, t) \, du - \mu \tilde{n}. \quad (19)$$

Using the methods described in Daniels (1975) and Medlock and Kot (2003), the rate of spread c^*_{DC} given compact initial conditions is

$$c^*_{DC} = r \sqrt{\theta e^\theta \left(\frac{D_s}{\alpha_s} + \frac{D_i}{\alpha_i} \right)}, \quad (20)$$
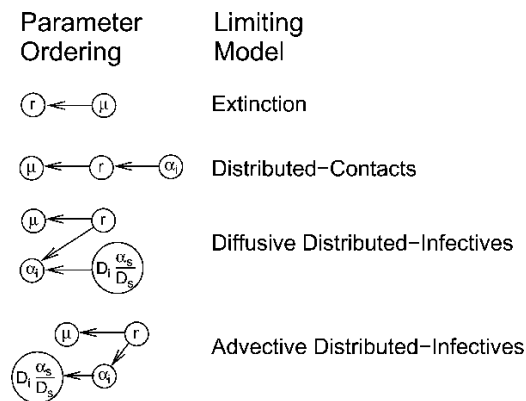

Fig. 2 Partial orderings describing the parameter relationships of the four asymptotic limits of the restricted-movement model. Arrows point from larger parameters to smaller parameters. For instance, if $r < \mu$, the transmission chain dies out, leading to extinction of the disease.

where θ solves

$$(1 - \theta)\, e^{\theta/2} = \frac{\mu}{r}. \tag{21}$$

In the special case of $\mu = 0$,

$$c_{DC}^* = r \sqrt{e \left(\frac{D_s}{\alpha_s} + \frac{D_i}{\alpha_i} \right)}, \tag{22}$$

where $e \approx 2.7$.

3.2. Diffusive distributed-infectives limit

When disease transmission is rapid ($r \gg \alpha_i$), transmission often occurs before an individual's position has relaxed to equilibrium. If diffusion is much faster than homeward attraction ($D_i \alpha_s / D_s \gg \alpha_i$), the movement of each individual is approximately independent of its home. If we apply this assumption and integrate over all homes, we find

$$\frac{\partial \overline{n}}{\partial t} = D_i \frac{\partial^2 \overline{n}}{\partial x^2} + (r - \mu) \overline{n}, \quad \text{where} \quad \overline{n}(x, t) = \int_{-\infty}^{\infty} n(x, x_h, t)\, dx_h. \tag{23}$$

This diffusion equation is a common description of the distributed-infectives model (Medlock and Kot, 2003). The asymptotic speed given compact initial conditions is

$$c_{DI}^* = 2\sqrt{D_i (r - \mu)}. \tag{24}$$

3.3. Advective distributed-infectives limit

When disease transmission is rapid ($r \gg \alpha_i$) but diffusion effects are weak ($D_i \alpha_s / D_s \ll \alpha_i$), advection governs dispersal. Because of the dominance of advection, we refer to this as the advective distributed-infectives model. The calculation of an asymptotic spread rate c_{ADI}^* is more challenging in the advective distributed-infectives case than in the previously studied cases. Dimensional analysis in the case of $D_i = 0$ shows

$$c_{ADI}^* = \alpha_i \sqrt{\frac{D_s}{\alpha_s}}\; f\left(\frac{r}{\alpha_i}, \frac{\mu}{\alpha_i} \right), \tag{25}$$

where f is an unknown function. One ad hoc solution method that seems to give reasonable estimates in the absence of removal ($\mu = 0$) is to solve Eq. (14) using the ansatz $\omega^* = 4c^*$. This ansatz is the asymptotic condition for there to be a single-critical point of the integrand of Eq. (16) within the interval $(0, 1)$, and is an approximate condition for minimization of Eq. (16) when ω is large. This leads to the solution

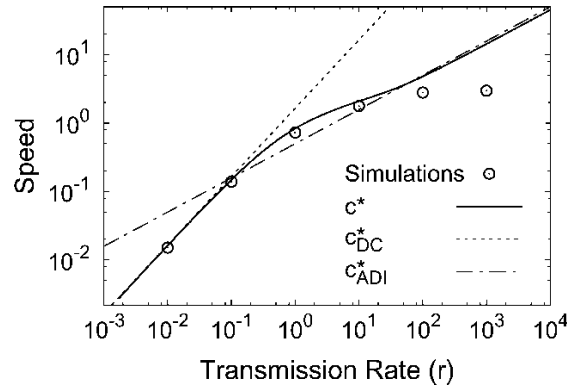$$c_{ADI}^* = \frac{1}{2} \sqrt{r \alpha_i \frac{D_s}{\alpha_s}}. \tag{26}$$

Fig. 3 Speeds c^* in the advective distributed-infectives limit ($D_i = 0$) and in the absence of removal ($\mu = 0$) compared to speeds observed in simulations. The open circles represent simulation speeds, calculated from 1000 runs, each up to 2 million infected individuals. For small transmission rates, speeds observed in individual-based simulations agree with predicted speed c^* and the distributed-contacts approximation. For large transmission rates, the speed of spread observed in individual-based simulations is dramatically slower than the minimum speed c^*, possibly due to the slow convergence of the simulations. Also, the minimum speed was slightly slower than the advective distributed-infectives approximation, Eq. (26). Parameters: $D_s = \alpha_s = \alpha_i = 1$.

However, Fig. 3 suggests that this approximation is strictly greater than c^* in the limit of rapid transmission ($r \gg \alpha_i$). The difficulty in computing the speed of the advective distributed-infectives limit may be because the non-local term appears to make non-vanishing contributions to $\hat{b}(c, \omega)$ in regions of solution of Eqs. (14) and (15).

4. Individual-based simulation

Here we compare the results of our mathematical analysis to individual-based simulations of the transmission process. The simulation methods are described in the Appendix.

The median spatial position of the epidemic at a given time was approximated using the empirical distribution of the furthest-forward observed individual from an ensemble of 1000 simulation runs. The speed is calculated by least-squares interpolation through the median epidemic positions (see Fig. 4). The simluation code is available on request.

Observations of spatial spread by individual-based simulation experiments generally coincided with the minimum speeds calculated from Eqs. (14) and (15) (see Figs. 5 and 6). Observed speeds were around 90% of the minimum speeds c^* by the time the infected population reached 2 million individuals. This prediction agrees with the previous simulation results of Snyder (2003) and Kot et al. (2004). Approaches based on Eqs. (14) and (15) are far more computationally efficient than individual-based simulations, and can obtain solutions in a matter of seconds rather than hours.
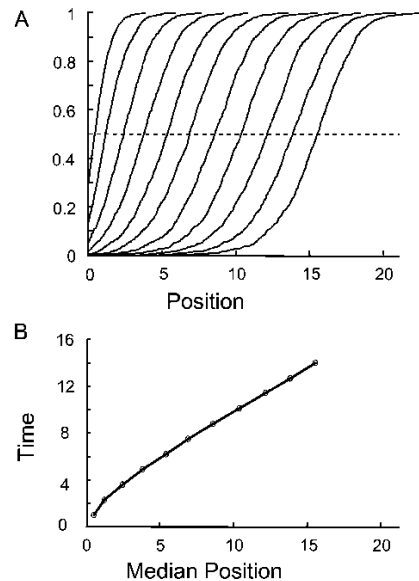
Fig. 4 An example of the numerical calculation of the median asymptotic speed from individual-based simulations. (A) Empirical distributions of the furthest-forward observed individuals, every 1.3 time units, accumulated from 1000 simulation runs, and (B) the median positions. The speed is approximated by least-squares interpolation of the linear portion of the median position curve. Parameters: $D_i = D_s = \alpha_i = \alpha_s = r = 1$, $\mu = 0$.

There is a significant discrepancy between the mathematical and simulation methods in the advective distributed-infectives limit. Simulation experiments demonstrated that speeds could be orders of magnitude slower than asymptotic prediction of the minimum wave speed c^* (see Fig. 3). Observed speeds decayed at a rate proportional to α_i. This did not accord with the the square-root dependence predicted by Eq. (26), which was derived using an ad hoc ansatz. Careful inspection of simulation results, however, suggests that epidemics were still accelerating at the end of simulation runs. It was likely that fronts had not reached their asymptotic spread rates before time and memory constraints stopped simulations at 2 million infected individuals. Nonetheless, if the spread is still accelerating after more than 2 million individuals have been infected, the asymptotic speed is probably not a practical upper bound in any realistic epidemiological scenario. Further research with particular emphasis on accelerating fronts is needed. When an advective distributed-infectives limit is considered most appropriate, we currently recommend that individual-based models be used, at least until a more efficient alternative is developed.

5. Discussion

In this paper we have formulated the restricted-movement model to describe spatial patterns of disease transmission. The restricted-movement model differs from
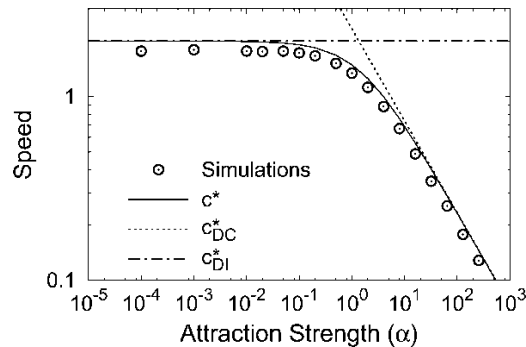
Fig. 5 The observed speed in individual-based simulations as a function of attraction strength $\alpha = \alpha_i = \alpha_s$. The relaxation time for individual movement is proportional to $1/\alpha_i$. For long relaxation times, the dispersal process is dominated by the distributed-infectives component. For short relaxation times, speeds agree with the distributed-contacts model's prediction, Eq. (20). The simulation results are close to the minimum speed c^* over the range of α. Parameters: $D_i = D_s = 1$, $r = 1$, $\mu = 0$.

existing models by describing individual movement relative to a "home" location to which individuals return sporadically. The restricted-movement model also unifies the distributed-infectives and distributed-contacts models in a common framework and further illuminates their relationships. When infected individuals return home rapidly, speeds in the restricted-movement model coincide with those of the distributed-contacts model. Conversely, when infected individuals return home very slowly relative to both diffusion and transmission, rates of spread in the restricted-movement model coincide with those of the diffusive distributed-infectives model. In the distributed-contacts and diffusive distributed-infectives limits, the asymptotic rates of spread can be calculated from the simple expressions we have formulated.

An imprecise approximation in the advective distributed-infectives limit is also given, but this limit requires further study. In the advective limit, the dispersal
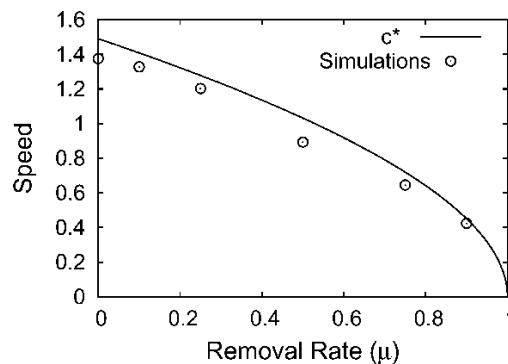

Fig. 6 The speeds observed in individual-based simulations as a function of removal rate μ, compared with minimum speeds c^*. By the completion of simulations, median simulation speeds have reached roughly 90% of the predicted speeds. Parameters: $D_s = D_i = 1$, $\alpha_s = \alpha_i = 1$, $r = 1$.

process is closely related to the "velocity jump process" of Othmer et al. (1988). The velocity jump process is motivated by the "run and tumble movement" of flagellated bacteria such as *E. coli*. This process describes the movement of an organism that alternately "runs" at a constant velocity and then "tumbles" to a new velocity. Alt (1980) derives a special case of the velocity jump process from biological assumptions and studies a diffusion approximation. Othmer et al. (1988) derives the velocity jump process from a generalization of the telegrapher's equation and then analyzes some special cases. Schwetlick (2000) shows the existence of traveling-wave solutions for the velocity jump process when the velocities of individuals are bounded and gives an expression for the minimum wave speed. Hillen and Othmer (2000) and Othmer and Hillen (2002) give a detailed study of diffusion approximations for the velocity jump process.

Individual-based models of social networks (Eubank et al., 2004) contain both static components, such as family contacts, and transient components, such as people sharing a crowded subway car. Under the restricted-movement model, transient components will govern the rate of spatial epidemic spread when transmission frequently occurs before the movement of an individual has relaxed to its equilibrium distributions. When many transmissions occur during relaxation, distributed-infectives models are most appropriate for describing spread. If transmissions seldom occur before relaxation, the distributed-contacts approach is the most appropriate. The boundary between these two limits can be approximated by equating Eqs. (24) and (20). In the specific case where removal is slow ($\mu \approx 0$), infection does not alter individual behavior ($D_s \alpha_i = D_i \alpha_s$), and individuals return home every night ($\alpha_i = 1$), the distributed-infectives model must be considered when there are more than 0.7 transmissions per day per individual. For example, smallpox and measles are transmitted more than once a day on average, and are likely to require distributed-infectives models, while scarlet fever is transmitted less than 0.5 times a day, suggesting a distributed-contacts model may be adequate (Anderson and May, 1991; Fenner et al., 1988).

Our results for the restricted-movement model are robust to a greater or lesser extent when the underlying assumptions are relaxed. For instance, the generalization from 1 to 2 spatial dimensions may prolong the transient dynamics, but is not expected to effect our asymptotic results. The mean-field description of disease transmission implicitly assumes a large, dense population. Disease spread is likely to be slower in a sparse population with fewer contacts between susceptible and infected individuals. The accumulation of immune individuals may further slow the spread of disease. We have also assumed that transmission can only occur through close contact between individuals. We have not explored scenarios where transmission is facilitated exogenously by vectors or other environmental factors.

The Ornstein–Uhlenbeck process is a convenient assumption which is reasonable for many animal species. Our qualitative results should also hold for other empirically derived movement models. Consider alternative cases where infected individuals advect away from their point of infection for a fixed time, after which they are stationary for the duration of infection. In such cases, we can expect epidemic spread to correspond to an advective distributed-infectives model for fast transmission, but a distributed-contacts model for slow transmission.
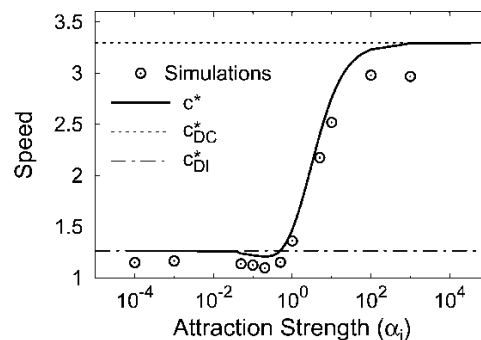
Fig. 7 Changes in epidemic speed depending on the attraction intensity α_i. With strong attraction ($\alpha_i \gg 1$), the distributed-contacts model provides a good approximation, while the diffusive distributed-infectives model provides the best approximations for weak attraction. Disease spread is slowest between distributed-contacts and distrubuted-infectives limits for $\alpha_i \approx 0.2$. Parameters: $D_i = 0.2, \mu = 0, r = 2, D_s/\alpha_s = 1$.

Greater biological realism can be achieved from the restricted-movement model by relaxing the assumptions of temporal, spatial, and demographic homogeneity. Temporal homogeneity can be relaxed to allow for daily and weekly movement cycles or aperiodic transients. Spatial homogeneity and isotropy can be loosened, particularly in two dimensions, to allow for spatial variation in population density and individual movement patterns. The current model captures some demographic heterogeneity by allowing infected and susceptible individuals to behave differently, but these classes themselves are assumed to be homogeneous. Demographic heterogeneity may be further explored by allowing population age structure and correlated movement of individuals. Each of these generalizations greatly increases the amount of biological information that can be incorporated into the restricted-movement model.

Our methods may also be of use in ecological studies of animal populations where individuals can exhibit behavioral biases in their movement. Density-dependence can be included by adding non-linear growth and mortality terms to Eq. (9). Such models provide an extension of diffusion models and might provide useful analytic results.

In conclusion, the restricted-movement model provides an improved approach to spatial epidemic modeling, and elucidates the relationship between popular distributed-contacts and distributed-infectives approaches. Along with the issues discussed above, future work may include applications of this theory to specific epidemic control problems.

Acknowledgements

Appendix: Individual-based simulation methods

Before describing the simulation procedure, it useful to lay out some notation, consistent with Evans et al. (2000). Let $E : b$ represent an exponential distribution with expectation b, let $N : a, b$ represent a Gauss distribution with mean a and standard deviation b, and let $U : x_h, y, t, D, \alpha$ represent the distribution of the position at time t of an individual with home x_h who started at position y at time 0, as given by Eq. (5). Also, the notation $x \sim X$ reads "the random variable x has distribution X".

Suppose there are currently $C(T)$ infected individuals enumerated $j = 1, 2, \ldots, C(T)$ at time T. For each individual j, we know that individual's home $x_h(j)$ and position $x(j)$ at some time $t(j) \leq T$.

The individual-based simulation is as follows. With uniform probability, randomly choose an individual j. Wait a time $\hat{t} = \min(\hat{t}_r, \hat{t}_\mu)$, where the time until the next transmission event $\hat{t}_r \sim E : 1/r C(T)$ and the time until the next removal event $\hat{t}_\mu \sim E : 1/\mu C(T)$. If the next event is a removal, then individual j is removed from the population, and $C(T + \hat{t}) = C(T) - 1$. If the next event is a transmission, individual j's current position $\hat{x} \sim U : x_h(j), x(j), \hat{t} + T - t(j), D_i, \alpha_i$ at time $T + \hat{t}$. The newly infected individual $I_{C(T)+1}$ has the same position $\hat{x}$ but his home $\hat{x}_h \sim N : \hat{x}, \sqrt{D_s/\alpha_s}$. The simulation is updated such that

$$x(j) = x(C(T) + 1) = \hat{x}, \tag{A.1}$$

$$t(j) = t(C(T) + 1) = T + \hat{t}, \tag{A.2}$$

$$x_h(C(T) + 1) = \hat{x}_h, \tag{A.3}$$

$$C(T + \hat{t}) = C(T) + 1. \tag{A.4}$$

Having updated the system, we now wait for the next transmission or removal event. The initial state for all simulations is one infected individual located at its home at the origin. Simulations stop when $C(T) = 0$ or $C(T)$ reaches the maximum allowed number, which, because of computational constraints, we limited to 2 million infected individuals.

C++ and Python code, suitable for use under GNU/Linux, is available on request.

One drawback of the simulation approach is that we do not have complete information about the simulation's state at any time after the first transmission event. During simulations, the position of the front $P(T)$ at time T is approximated as the position of the furthest-forward observed individual,

$$P(T + \hat{t}) = \max\{\hat{x}, P(T)\}. \tag{A.5}$$

This may overestimate the advance of the front, if the furthest-forward observation has retreated since last observed, or this may underestimate the advance, because the position of only 2 infected individuals is known precisely at time T. We have compared our method to simulations where complete snapshots of the population were calculated at specific time points. The results from both approaches agreed, but we found the snapshot approach was approximately 1.5 times slower.

References

Allen, L., Ernest, R., 2002. The impact of long-range dispersal on the rate of spread in population and epidemic models. In: Castillo-Chavez, C., Blower, S., van den Driessche, P., Kirschner, D., Yakubu, A.-A. (Eds.), Mathematical Approaches for Emerging and Reemerging Infectious Diseases: An Introduction. Springer, New York, pp. 183–197.

Alt, W., 1980. Biased random-walk models for chemotaxis and related diffusion approximations. J. Math. Biol. 9, 147–177.

Anderson, R.M., May, R.M., 1991. Infectious Diseases of Humans: Dynamics and Control. Oxford University Press, New York.

Arino, J., van den Driessche, P., 2003. A multi-city epidemic model. Math. Pop. Stud. 10, 175–193.

Bailey, N.T.J., 1975. The Mathematical Theory of Infectious Diseases, 2nd ed. Griffin, London.

Bauch, C.T., Galvani, A.P., 2003. Using network models to approximate spatial point-process models. Math. Biosci. 184, 101–114.

Bian, L., 2004. A conceptual framework for an individual-based spatially explicit epidemiological model. Environ. Plan. B-Plan. Design 31, 381–395.

Busenberg, S.N., Travis, C.C., 1983. Epidemic models with spatial spread due to population migration. J. Math. Biol. 16, 181–198.

Caraco, T., Glavanakov, S., Chen, G., Flaherty, J.E., Ohsumi, T.K., Szymanski, B.K., 2002. Stage-structured infection transmission and a spatial epidemic: A model for Lyme disease. Am. Natural. 160, 348–359.

Clark, J.S., Lewis, M., Horvath, L., 2001. Invasion by extremes: Population spread with variation in dispersal and reproduction. Am. Natural. 152, 204–224.

Daniels, H.E., 1975. The deterministic spread of a simple epidemic. In: Gani, J. (Ed.), Perspectives in Probability and Statistics: Papers in Honour of M. S. Bartlett on the Occasion of his Sixty-Fifth Birthday. Academic Press, London, pp. 373–386.

Doran, R.J., Laffan, S.W., 2005. Simulating the spatial dynamics of foot and mouth disease outbreaks in feral pigs and livestock in Queensland, Australia, using a susceptible-infected-recovered cellular automata model. Prev. Vet. Med. 70, 133–152.

Durrett, R., 1999. Stochastic spatial models. SIAM Rev. 41, 677–718.

Durrett, R., Levin, S., 1994. The importance of being discrete (and spatial). Theor. Pop. Biol. 46, 363–394.

Eubank, S., Guclu, H., Kumar, V.S.A., Marathe, M.V., Srinivasan, A., Toroczkai, Z., Wang, N., 2004. Modelling disease outbreaks in realistic urban social networks. Nature 429, 180–184.

Evans, M., Hastings, N., Peacock, B., 2000. Statistical Distributions, 2nd ed. Wiley, New York.

Fenner, F., Henderson, D.A., Arita, I., Jezek, Z., Ladnyi, I., 1988. Smallpox and Its Eradication. World Health Organization, Geneva.

Fife, P.C., 1979. Mathematical Aspects of Reacting and Diffusing Systems. Lecture Notes in Biomathematics. Springer-Verlag, New York.

Filipe, J.A.N., Maule, M.M., 2003. Analytical methods for predicting the behaviour of population models with general spatial interactions. Math. Biosci. 183, 15–35.

Fuks, H., Lawniczak, A.T., 2001. Individual-based lattice model for spatial spread of epidemics. Discrete Dyn. Nat. Soc. 6, 191–200.

Goel, N.S., Richter-Dyn, N., 1974. Stochastic Models in Biology. Academic Press, New York.

Hadeler, K.P., 2003. The role of migration and contact distributions in epidemic spread. In: Banks, H.T., Castillo-Chavez, C. (Eds.), Bioterrorism: Mathematical Modeling Applications in Homeland Security. SIAM, Philadelphia, pp. 199–210.

Hillen, T., Othmer, H.G., 2000. The diffusion limit of transport equations derived from velocity-jump processes. SIAM J. Appl. Math. 61, 751–775.

Keeling, M.J., Gilligan, C.A., 2000. Bubonic plague: A metapopulation model of a zoonosis. Proc. R. Soc. Lond. B 267, 2219–2230.

Kendall, D.G., 1965. Mathematical models of the spread of infection. In Mathematics and Computer Science in Biology and Medicine. H. M. Stationary Office, London, pp. 213–225.

Kot, M., 2001. Elements of Mathematical Ecology. Cambridge University Press, New York.

Kot, M., Medlock, J., Reluga, T., Walton, D.B., 2004. Stochasticity, invasions, and branching random walks. Theor. Pop. Biol. 66, 175–184.

Lewis, M.A., 2000. Spread rate for a nonlinear stochastic invasion. J. Math. Biol. 41, 430–454.

Lewis, M.A., Pacala, S., 2000. Modeling and analysis of stochastic invasion processes. J. Math. Biol. 41, 387–429.

Lloyd, A.L., Jansen, V.A.A., 2004. Spatiotemporal dynamics of epidemics: Synchrony in metapop-ulation models. Math. Biosci. 188, 1–16.

McKean, H.P., 1975. Application of Brownian motion to the equation of Kolmogorov–Petrovskii–Piskunov. Commun. Pure Appl. Math. 28, 323–331.

Medlock, J., Kot, M., 2003. Spreading disease: Integro-differential equations old and new. Math. Biosci. 184, 201–222.

Méndez, V., 1998. Epidemic models with an infected-infectious period. Phys. Rev. E 57, 3622–3624.

Metz, J.A.J., Mollison, D., van den Bosch, F., 1999. The Dynamics of Invasion Waves. Technical Report IR-99-039, International Institute for Applied Systems Analysis. Laxenburg, Austria.

Metz, J.A.J., van den Bosch, F., 1995. Velocities of epidemic spread. In: Mollison, D. (Ed.), Epidemic Models: Their Structure and Relation to Data. Cambridge University Press, Cambridge, UK, pp. 150–186.

Meyers, L.A., Pourbohloul, B., Newman, M.E.J., Skowronski, D.M., Brunham, R.C., 2005. Net-work theory and SARS: Predicting outbreak diversity. J. Theor. Biol. 232, 71–81.

Mollison, D., 1972. The rate of spatial propagation of simple epidemics. In: Proceedings of the 6th Berkeley Symposium on Mathematical Statistics and Probability, vol. 3. University of California Press, Berkeley, CA, pp. 579–614.

Mollison, D., 1977. Spatial contact models for ecological and epidemic spread. J. R. Stat. Soc. B 39, 283–326.

Mollison, D., 1991. Dependence of epidemic and population velocities on basic parameters. Math. Biosci. 107, 255–287.

Newman, M.E.J., 2002. Spread of epidemic disease on networks. Phys. Rev. E 66, 016128.

Noble, J.V., 1974. Geographic and temporal development of plagues. Nature 250, 726–729.

Othmer, H.G., Dunbar, S.R., Alt, W., 1988. Models of dispersal in biological-systems. J. Math. Biol. 26, 263–298.

Othmer, H.G., Hillen, T., 2002. The diffusion limit of transport equations II: Chemotaxis equa-tions. SIAM J. Appl. Math. 62, 1222–1250.

Read, J.M., Keeling, M.J., 2003. Disease evolution on networks: the role of contact structure. Proc. R. Soc. Lond. B 270, 699–708.

Riley, S., Fraser, C., Donnelly, C.A., Ghani, A.C., Abu-Raddad, L.J., Hedley, A.J., Leung, G.M., Ho, L.M., Lam, T.H., Thach, T.Q., Chau, P., Chan, K.P., Leung, P.Y., Tsang, T., Ho, W., Lee, K.H., Lau, E.M.C., Ferguson, N.M., Anderson, R.M., 2003. Transmission dynamics of the etiological agent of SARS in Hong Kong: Impact of public health interventions. Science 300, 1961–1966.

Schinazi, R., 1996. On an interacting particle system modeling an epidemic. J. Math. Biol. 34, 915–925.

Schwetlick, H.R., 2000. Travelling fronts for multidimensional nonlinear transport equations. Ann. Inst. Henri Poincare Phys. Theor. 17, 523–550.

Snyder, R.E., 2003. How demographic stochasticity can slow biological invasions. Ecology 84, 1333–1339.

Thomson, N.A., Ellner, S.P., 2003. Pair-edge approximation for heterogeneous lattice population models. Theor. Pop. Biol. 64, 271–280.

Uhlenbeck, G.E., Ornstein, L.S., 1930. On the theory of the Brownian motion. Phys. Rev. 36, 823–841.

van den Bosch, F., Metz, J., Zadoks, J., 1999. Pandemics of focal plant disease, a model. Phytopathology 89, 495–505.

van den Bosch, F., Verhaar, M., Buiel, A., Hoogkamer,W., Zadoks, J., 1990. Focus expan-sion in plant disease. IV: Expansion rates in mixtures of resistant and susceptible hosts. Phytopathology 80, 598–602.

van den Bosch, F., Zadoks, J., Metz, J., 1988. Focus expansion in plant disease. I: The constant rate of focus expansion. Phytopathology 78, 54–58.